Journal of Engineering Mathematics **40:** 77–90, 2001.

The effect of viscosity on the transient free-surface waves in a two-dimensional tank

G. X. WU, R. EATOCK TAYLOR[1] and D. M. GREAVES
Department of Mechanical Engineering, University College London, Torrington Place, London WC1 7JE, UK
[1]*Department of Engineering Science, University of Oxford, Parks Road, Oxford OX1 3PJ, UK*

Received 15 June 1999; accepted in revised form 27 March 2000

Abstract. The paper attempts to develop some understanding of the interaction between viscous flow and a free surface by analysing the unsteady flow in an idealised two-dimensional rectangular tank. The mathematical model used is based on the linearized Navier-Stokes equations which are solved by use of the Laplace transform. Various results are provided to show the effect of viscosity on the free surface waves.

Key words: free surface, sloshing waves, viscosity

1. Introduction

Water waves are primarily dominated by gravity and in the absence of solid boundaries viscosity usually has very little effect on the flow over a short period in time or over a short distance in space [1, Section 3.5]. In other words, the effects of viscosity may become important only after many wave periods or after many wavelengths. It is quite common, therefore, that free-surface flows associated with water waves are analysed by the velocity potential theory. The problem becomes somewhat different when a wave encounters a body in its path, because of the sheared flow created by the body surface. But even in that case it is usually a common practice to deal with the free-surface effects and viscous effects separately. A typical example is linear wave interaction with an offshore structure. The interaction between the wave and the body can be analysed by either wave-diffraction theory without viscosity or by viscous-flow theory without the free-surface effect, depending on the ratios of the characteristic dimension of the body to the wavelength and the wave amplitude [2].

Cases, however, do arise where the combined effect of the free surface and viscosity is important, some of which have been highlighted by Yeung and Yu [3]. A noteworthy case is the flow near the waterline of a floating body, *i.e.*, at the intersection of the body surface and the free surface. Another example is the free surface flow of highly viscous fluid. The purpose of the present analysis is to derive some understanding of how the free surface interacts with the viscosity by considering a geometrically simple fluid domain, an idealised two-dimensional rectangular tank. As a starting point, common in potential flow analysis, it is assumed that disturbance of the fluid is small and the flow is governed by the linearized Navier-Stokes (NS) equations. The justification and limitations of such an approximation have been discussed by Mei [4, Chapter 8]. The analysis there is, however, based on the framework of boundary-layer theory. Here the viscous effect is taken into account in the entire fluid domain.

One difficulty in combined free-surface and viscous analysis lies at the intersection of the body surface and the free surface. Take a fixed body as an example: the no-slip condition in

the NS equations suggests that the fluid particle there should remain stationary, but it can be observed experimentally that fluid moves up and down along the body surface. This difficulty was in fact mentioned by Lamb [5, Article 327], and resolving it requires extensive experimental study such as that undertaken in [6]. Our current understanding of the flow structure near the intersection is still limited and many methods used to deal with the intersection are not entirely satisfactory. A commonly used scheme for water wave/structure interaction is based on two steps: (1) the NS equations are solved with the no-slip condition imposed on the body surface and (2) the motion of the intersection point is tracked through interpolation from the points on the free surface and near the intersection. This procedure has some clear defects. To ensure the result from the interpolation is accurate enough, the points used must be as close as possible to the intersection. However, if these points are sufficiently close to the body surface (for example when an extremely fine mesh is used in this region), the result will be the same as that based on the no-slip condition. Because of this difficulty, the analysis in this work remains modest. The no-slip condition on the body is replaced by a no-shear-force condition. The intention here is to show how the free surface will interact with the viscous flow, and results based on this model would be useful for this purpose. Indeed it was argued in [7] that the condition on the side walls may have little effect on the wave when analysing Faraday's instability. Furthermore, the equivalent of a zero shear force condition on the side walls was also used by Loh and Rasmussen [8], who solved the full Navier-Stokes equations for this problem based on the finite-difference method. The present analytical solution of the flow in an oscillating tank therefore has an additional use for validation purposes. Having said that, it should be noted that we cannot justify the condition used on the body surface yet. Whether the solution obtained reflects the physical reality is not entirely clear. Tentatively, it appears that the solution may be more physical at low Reynolds number than at high Reynolds number, because in the latter case, the effect of shear stresses may be more important on the body surface than in the fluid domain.

2. Mathematical formulation

We consider the problem of viscous fluid flow in a rectangular tank of length l. A Cartesian coordinate system $O - xz$ is defined so that its origin is located at the centre of the mean free surface and z points upwards. When the disturbance to the liquid is small, its motion may be described by the following linearised Navier-Stokes and continuity equations

$$\frac{\partial u}{\partial t} = -\frac{1}{\rho}\frac{\partial p}{\partial x} + \nu\nabla^2 u, \quad \frac{\partial w}{\partial t} = -\frac{1}{\rho}\frac{\partial p}{\partial z} + \nu\nabla^2 w, \quad \frac{\partial u}{\partial x} + \frac{\partial w}{\partial z} = 0, \tag{1a,b,c}$$

where u and w are the velocity components in the x and z directions respectively, p is the pressure, ρ is the density and ν is the kinematic viscosity. In Equation (1b) the term due to gravity has been included in the pressure.

On the mean free surface $z = 0$, the boundary conditions can be written as [4]

$$\eta_t = w, \quad p/\rho = g\eta + 2\nu w_z, \quad u_z + w_x = 0, \tag{2a,b,c}$$

where η is the wave elevation, g is the acceleration due to gravity and all the subscripts indicate derivatives.

On the solid boundary, we adopt the condition which assumes that the normal velocity components of the fluid particle and the body surface are the same and the frictional force is zero. It follows that

$$u = U_0(t), \quad u_z + w_x = 0 \quad \text{at} \quad x = \pm l/2, \tag{3a}$$

$$w = W_0(t), \quad u_z + w_x = 0 \quad \text{at} \quad (z = -d) \tag{3b}$$

where U_0 and W_0 are the horizontal and vertical velocity components of the tank. In this analysis, we assume that motion starts smoothly, which means $U_0(0) = W_0(0) = 0$.

We now introduce

$$u = \phi_x - \psi_z, \quad w = \phi_z + \psi_x, \tag{4a,b}$$

which in fact implies $p = -\rho\partial\phi/\partial t$. The governing equations in (1) become [5, Article 349]

$$\nabla^2\phi = 0, \quad \psi_t = \nu\nabla^2\psi \tag{5a,b}$$

in the fluid domain, and the boundary conditions in (2) and (3) become

$$\psi_{xx} - \psi_{zz} + 2\phi_{xz} = 0, \quad \phi_{tt} + g(\phi_z + \psi_x) + 2\nu(\phi_{zzt} + \psi_{xzt}) = 0 \tag{6a,b}$$

on $z = 0$, and

$$\phi_x = U_0, \quad \psi = 0 \qquad \text{at} \quad x = \pm l/2 \tag{7a}$$

$$\phi_z = W_0, \quad \psi = 0 \qquad \text{at} \quad z = -d. \tag{7b}$$

3. Solution procedure

We now introduce the Laplace transform with respect to time:

$$f^*(\lambda) = \int_0^\infty f(t)\, \mathrm{e}^{-\lambda t}\, \mathrm{d}t. \tag{8}$$

Equations (5–7) then become

$$\nabla^2\phi^* = 0, \quad \lambda\psi^* = \nu\nabla^2\psi^* \tag{9a,b}$$

in the fluid domain,

$$\psi^*_{xx} - \psi^*_{zz} + 2\phi^*_{xz} = 0, \quad \lambda^2\phi^* + g(\phi^*_z + \psi^*_x) + 2\lambda\nu(\phi^*_{zz} + \psi^*_{xz}) = -g\eta_0 \tag{10a,b}$$

on $z = 0$, where η_0 is the initial wave elevation, and

$$\phi^*_x = U^*_0, \quad \psi^* = 0 \quad \text{at} \quad x = \pm l/2 \tag{11a}$$

$$\phi^*_z = W^*_0, \quad \psi^* = 0 \quad \text{at} \quad z = -d. \tag{11b}$$

Equations (9) and (11) clearly allow us to write

$$\phi^* = U^*_0 x + W^*_0 z + \sum_{n=1}^{\infty} A_n \frac{\cosh\, k_n(z+d)}{\cosh\, k_n d} \cos\, k_n(x + l/2), \tag{12a}$$

$$\psi^* = \sum_{n=1}^{\infty} B_n \frac{\sinh\, \alpha_n(z+d)}{\cosh\, \alpha_n d} \sin\, k_n(x + l/2), \tag{12b}$$

where

$$k_n = n\pi/l, \quad \alpha_n = \sqrt{k_n^2 + \lambda/\nu}. \tag{13a,b}$$

Substituting Equations (12) in (10) we obtain

$$2k_n^2 \tanh(k_n d) A_n + (\alpha_n^2 + k_n^2) \tanh(\alpha_n d) B_n = 0, \tag{14a}$$

$$(\lambda^2 + k_n g \tanh k_n d + 2\nu\lambda k_n^2) A_n + (k_n g \tanh \alpha_n d + 2\nu k_n \alpha_n \lambda) B_n = -a_n, \tag{14b}$$

where

$$\begin{aligned} a_n &= \frac{2}{l}\int_{-l/2}^{l/2} (g\eta_0 + \lambda^2 U_0^* x + g W_0^*) \cos k_n(x + l/2)\, \mathrm{d}x \\ &= -\frac{2\lambda^2 U_0^*}{l k_n^2}[1 - (-1)^n] + \frac{2g}{l}\int_{-l/2}^{l/2} \eta_0 \cos k_n(x + l/2)\, \mathrm{d}x. \end{aligned} \tag{15}$$

The solution of Equations (14) can be found as

$$A_n = a_n \frac{\alpha_n^2 + k_n^2}{C_n} \tanh \alpha_n d, \quad B_n = -a_n \frac{2k_n^2}{C_n} \tanh k_n d \tag{16a,b}$$

where

$$\begin{aligned} C_n &= 2k_n^2 \tanh k_n d(k_n g \tanh \alpha_n d + 2\nu k_n \alpha_n \lambda) \\ &\quad -(\alpha_n^2 + k_n^2) \tanh \alpha_n d(\lambda^2 + k_n g \tanh k_n d + 2\nu k_n^2 \lambda) \\ &= -\lambda/\nu[\lambda^2 \tanh \alpha_n d + 4k_n^2 \nu\lambda \tanh \alpha_n d + g k_n \tanh \alpha_n d \tanh k_n d \\ &\quad +4\nu^2 k_n^3 (k_n \tanh \alpha_n d - \alpha_n \tanh k_n d)]. \end{aligned} \tag{17}$$

Thus

$$\phi = U_0 x + W_0 z + \frac{1}{2\pi \mathrm{i}} \sum_{n=1}^{\infty} \int_\Gamma \frac{\alpha_n^2 + k_n^2}{C_n} a_n \tanh \alpha_n d \mathrm{e}^{\lambda t}\, \mathrm{d}\lambda \frac{\cosh k_n(z + d)}{\cosh k_n d} \cos k_n(x + l/2), \tag{18a}$$

$$\psi = -\frac{1}{2\pi \mathrm{i}} \sum_{n=1}^{\infty} \int_\Gamma \frac{2k_n^2 a_n}{C_n} \frac{\sinh \alpha_n(z + d)}{\cosh \alpha_n d} \mathrm{e}^{\lambda t}\, \mathrm{d}\lambda \tanh k_n d \sin k_n(x + l/2), \tag{18b}$$

where the integration path Γ is taken so that all the poles of the integrand are on its left hand side.

The wave elevation can be obtained from

$$\begin{aligned} \eta &= \frac{1}{g}[-\phi_t - 2\nu(\phi_{zz} + \psi_{xz})]_{z=0} \\ &= -\frac{x}{g}\frac{dU_0}{dt} + \frac{1}{2\pi \mathrm{i} g} \sum_{n=1}^{\infty} \int_\Gamma \frac{-(\alpha_n^2 + k_n^2) \tanh \alpha_n d(\lambda + 2\nu k_n^2) + 4\nu k_n^3 \alpha_n \tanh k_n d}{C_n} a_n \mathrm{e}^{\lambda t}\, \mathrm{d}\lambda \\ &\quad \times \cos k_n(x + l/2). \end{aligned}$$

Since

$$-(\alpha_n^2 + k_n^2)\ \tanh\ \alpha_n d(\lambda + 2\nu k_n^2) + 4\nu k_n^3 \alpha_n\ \tanh\ k_n d$$

$$= \frac{1}{\lambda}(C_n + \lambda g k_n\ \tanh\ k_n d\ \tanh\ \alpha_n d/\nu),$$

we have

$$\eta = -\frac{x}{g}\frac{dU_0}{dt} + \frac{1}{2\pi \mathrm{i} g}\int_\Gamma \frac{\mathrm{e}^{\lambda t}}{\lambda}\sum_{n=1}^{\infty} a_n\ \cos\ k_n(x + l/2)\ \mathrm{d}\lambda$$

$$+\frac{1}{2\pi \mathrm{i}\nu}\sum_{n=1}^{\infty} k_n\ \tanh\ k_n d\int_\Gamma \frac{a_n\ \tanh\ \alpha_n d}{C_n}\mathrm{e}^{\lambda t}\mathrm{d}\lambda\ \cos\ k_n(x + l/2).$$

Equation (15) shows that a_n are the coefficients of the cosine series of $g\eta_0 + \lambda^2 U_0^* x$. Thus

$$\begin{aligned}\eta\ &=\ -\frac{x}{g}\frac{dU_0}{dt} + \frac{1}{2\pi \mathrm{i} g}\int_\Gamma \frac{\mathrm{e}^{\lambda t}}{\lambda}(g\eta_0 + \lambda^2 U_0^* x)\ \mathrm{d}\lambda \\ &\quad +\frac{1}{2\pi \mathrm{i}\nu}\sum_{n=1}^{\infty} k_n\ \tanh\ k_n d\int_\Gamma \frac{a_n\ \tanh\ \alpha_n d}{C_n}\mathrm{e}^{\lambda t}\ \mathrm{d}\lambda\ \cos\ k_n(x + l/2) \qquad (19) \\ &=\ \eta_0 + \frac{1}{2\pi \mathrm{i}\nu}\sum_{n=1}^{\infty} k_n\ \tanh\ k_n d\int_\Gamma \frac{a_n\ \tanh\ \alpha_n d}{C_n}\mathrm{e}^{\lambda t}\ \mathrm{d}\lambda\ \cos\ k_n(x + l/2)\end{aligned}$$

One point worth noting is that this equation with (15) shows that the wave elevation does not depend on the vertical motion of the tank. This is a result of linearisation. In fact, it is known that the free surface wave generated by the vertical motion is not always stable. The instability of this so-called Faraday wave can be captured by the potential flow when the product term of the vertical acceleration with the surface elevation is included in the linear analysis [9]. The effect of viscosity on the stability was recently investigated by Cerda and Tirapegui [7]. Faraday waves, however, are beyond the main interest of the present work.

4. Results

4.1. A STATIONARY TANK

We first consider the case of a stationary tank with an initial wave elevation. Let

$$\eta_0 = a\ \cos\ k_2(x + l/2), \qquad (20)$$

where k_2 is given in Equation (13a). The solution for this case based on both the linearized and the second order potential flow theory has been given by Wu and Eatock Taylor [10]. Here Equation (15) gives

$$n = 2: \quad a_n = ga; \quad n \neq 2: \quad a_n = 0 \qquad (21)$$

and Equation (19) becomes

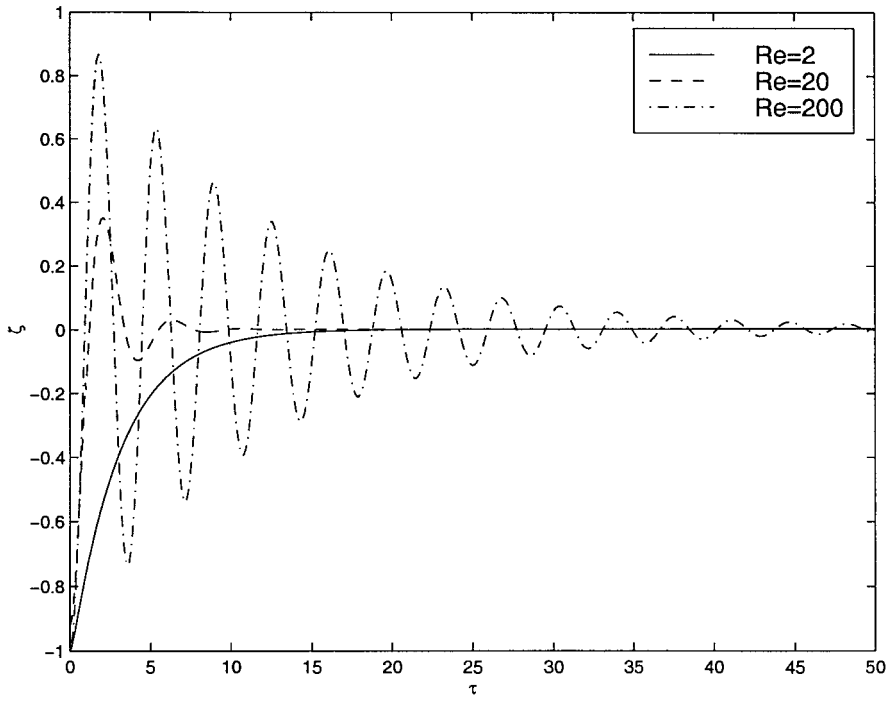

Figure 1. Decay of wave elevation at different Reynolds numbers.

$$\eta = \eta_0 + \frac{\eta_0 g k_2 \tanh k_2 d}{2\pi \nu \mathrm{i}} \int_\Gamma \frac{\tanh \alpha_2 d}{C_2} \mathrm{e}^{\lambda t} \, \mathrm{d}\lambda. \tag{22}$$

From Equation (17), the only zero of C_2 which can be found analytically is $\lambda = 0$. Other zeros have to be found numerically in the complex plane. This makes the direct application of the Cauchy theorem difficult. In the following analysis for finite water depth, the results are obtained by numerical integration of Equation (22) along a vertical line with $\mathfrak{Re}(\lambda) > 0$, based on the trapezoidal method. There is no particular difficulty in the computation provided a sufficiently small step is used, so that its further reduction will not lead to graphically visible differences. Generally the step depends on t and the larger t is, the smaller the step should be. But this does not cause any real computational problem as each calculation takes only a few seconds. Figure 1 gives results for the wave elevation $\zeta = \eta/a$ at $x = 0$ against time $\tau = t\sqrt{g/d}$ at different Reynolds number, defined as $\mathrm{Re} = d\sqrt{gd}/\nu$, in a tank with $l = 2d$. The figure clearly shows that the wave will decay to zero straight away at lower Reynolds number and oscillate with decaying amplitude at higher Reynolds number, which agrees with the physics of the problem.

An alternative approach is possible if the water is sufficiently deep, $k_2 d \to \infty$. It may be shown that in the limit:

$$\tanh k_2 d \to 1; \quad \tanh \alpha_2 d \to 1.$$

The latter limit holds even when $\alpha_2 d$ is complex, as long as $\mathfrak{Re}(\alpha_2) \neq 0$. Under these conditions Equation (17) yields:

$$C_2 = 2k_2^2(k_2 g + 2\nu k_2 \alpha_2 \lambda) - (\alpha_2^2 + k_2^2)(\lambda^2 + g k_2 + 2\nu k_2^2 \lambda).$$

It is convenient to define the following dimensionless parameters:

$$\kappa = \frac{g}{\nu^2 k_2^3}; \quad \sigma = \frac{\lambda}{\nu k_2^2}.$$

The expression for the wave elevation, Equation (22), can then be written in the form:

$$\frac{\eta(t)}{\eta_0} = 1 - \frac{\kappa}{2\pi \mathrm{i}} \int_\Gamma \frac{\mathrm{e}^{\sigma \nu k_2^2 t}\, \mathrm{d}\sigma}{\sigma[(\sigma+2)^2 - 4(\sigma+1)^{\frac{1}{2}} + \kappa]}. \tag{23}$$

Thus

$$\frac{\eta(t)}{\eta_0} = 1 - \kappa \mathrm{e}^{-\nu k_2^2 t} f(\nu k_2^2 t), \tag{24}$$

where $f(t)$ is the inverse Laplace transform of the function

$$F(s) = \frac{1}{(s-1)[(s+1)^2 - 4s^{\frac{1}{2}} + \kappa]}. \tag{25}$$

We have here replaced $(\sigma + 1)$ by s, thereby introducing the term $\mathrm{e}^{-\nu k_2^2 t}$ in Equation (24).

It may be shown that, provided $\kappa > 0{\cdot}5814122$ (see the appendix), the function in the square brackets may be written in partial fractions such that

$$F(s) = \frac{1}{(s-1)} \left[\frac{A_1}{\sqrt{s} - \gamma_1} + \frac{\bar{A}_1}{\sqrt{s} - \bar{\gamma}_1} + \frac{A_2}{\sqrt{s} - \gamma_2} + \frac{\bar{A}_2}{\sqrt{s} - \bar{\gamma}_2} \right]. \tag{26}$$

Here the overbar denotes complex conjugate, and γ_1, $\bar{\gamma}_1$, γ_2, $\bar{\gamma}_2$ are the roots of the equation

$$(x^2+1)^2 - 4x + \kappa = 0. \tag{27}$$

The coefficients A_1 and A_2, which may be obtained by equating powers of x in the partial fraction expansion, are given in the Appendix.

The inverse Laplace transform of terms arising from the four quotients in Equation (26) is in the form of the complex error function [11, Equations 29.3.42]:

$$\frac{1}{(s-1)(\sqrt{s}-a)} \to \frac{1}{1-a^2} \left\{ -a\mathrm{e}^{a^2 t} \mathrm{erfc}\left(-a\sqrt{t}\right) + \mathrm{e}^t [a + \mathrm{erf}(\sqrt{t})] \right\}$$

Hence the inverse transform may be written

$$f(t) = 2\mathfrak{Re} \sum_{i=1}^{2} \frac{A_i \left\{ -\gamma_i \mathrm{e}^{\gamma_i^2 t} \left[1 + \mathrm{erf}\left(\gamma_i \sqrt{t}\right) \right] + \mathrm{e}^t \left[\gamma_i + \mathrm{erf}\left(\sqrt{t}\right) \right] \right\}}{1 - \gamma_i^2} \tag{28}$$

In terms of the original variables, we can then write the wave elevation in the closed form:

$$\frac{\eta(t)}{\eta_0} = 1 - 2\kappa \mathfrak{Re} \sum_{i=1}^{2} \frac{A_i \left\{ -\gamma_i \mathrm{e}^{(-1+\gamma_i^2)\nu k_2^2 t} \left[1 + \mathrm{erf}\left(\gamma_i k_2 \sqrt{\nu t}\right) \right] + \gamma_i + \mathrm{erf}\left(k_2 \sqrt{\nu t}\right) \right\}}{1 - \gamma_i^2} \tag{29}$$

An approximation may be obtained when κ is sufficiently large. The Laplace transform in Equation (23) is then approximated by

$$F(\sigma) = \frac{1}{\sigma[(\sigma+2)^2 + \kappa]}. \tag{30}$$

The inverse transform is obtained from Equation 29.3.14 of Abramowitz and Stegun [11], leading to:

$$f(t) = \frac{\left[1 - \mathrm{e}^{-2t}\left(\cos\sqrt{\kappa}t + 2\sin\sqrt{\kappa}t/\sqrt{\kappa}\right)\right]}{(4+\kappa)}. \tag{31}$$

Substituting this in Equation (24) leads to the following closed form expression in terms of the original variables:

$$\frac{\eta(t)}{\eta_0} = 1 - \frac{1}{1 + 4\nu^2 k_2^3/g}\left[1 - \mathrm{e}^{-2\nu k_2^2 t}\left(\cos\sqrt{k_2 g}t + 2\nu k_2^2 \frac{\sin\sqrt{k_2 g}t}{\sqrt{k_2 g}}\right)\right] \tag{32}$$

Equation (32) shows that under the condition of large κ (which corresponds to large Reynolds number), the elevation decays in a very similar manner to an initially displaced, damped, single degree of freedom system which is subjected to step function forcing. The equivalent critical damping ratio is seen to be $2\nu k_2^2/\sqrt{k_2 g} = 2\kappa^{-\frac{1}{2}}$.

We can compare the results from the deep water analysis, Equation (24), and the subsequent approximation for large κ, Equation (32), with results from the finite water depth analysis for the stationary tank, Equation (22). First we note that for the case considered here $k_2 = 2\pi/l = \pi/d$. Hence with the definition of Re given following Equation (22), we have

$$\kappa = \frac{g}{\nu^2 k_2^3} = \frac{\mathrm{Re}^2}{\pi^3}.$$

For the values Re = 2, 20, 200 considered in Figure 1, the corresponding values of κ are 0·13, 12·9, 1290. The first of these is below the critical value stated above Equation (26), and we will not consider it further. For the other two cases, the equivalent critical damping ratios as defined above take the values 0·557 and 0·0557.

Figures 2a and 2b show time histories of the surface elevation ζ for Re = 20 and 200, respectively, plotted in the same way as Figure 1. The lines in the figures correspond to results based on the finite water depth analysis, Equation (22); the complete deep water analysis, Equation (29); and the approximate deep water analysis for large κ or Re, Equation (32). To evaluate Equation (29), the error function with complex argument was calculated using the Maple V mathematical program. It can be seen that the results from the deep water analysis of Equation (24) are indistinguishable from the complete analysis based on Equation (22); but the approximation for large κ is inaccurate in these two cases. The latter approximation slightly overestimates the damping, and in the case Re = 20, κ = 12·9, it leads to a noticeable offset at large t. (Equation (32) shows the value of this offset to be $4/(4+\kappa)$). Figure 2c compares the deep water analysis of Equation (29) with the large κ analysis for the case Re = 2000, corresponding to κ = 129006. Here the agreement is very close, as might be expected.

4.2. An oscillating tank

We next consider the case in which the tank undergoes the horizontal oscillation defined by

$$U_0(t) = \omega b \sin\omega t, \tag{33}$$

where b is the amplitude of the displacement and ω is the frequency. The initial free surface is assumed to be undisturbed, $\eta_0(x) = 0$. Equations (8) and (15) give

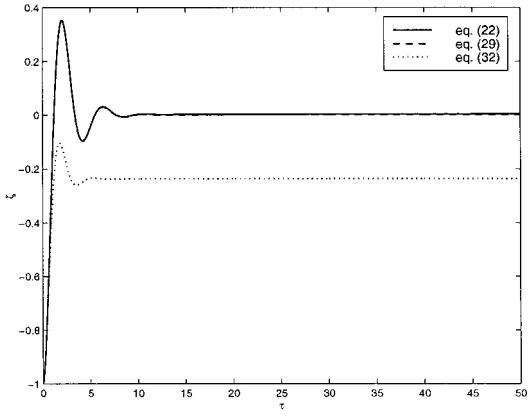

(2a) Re = 20

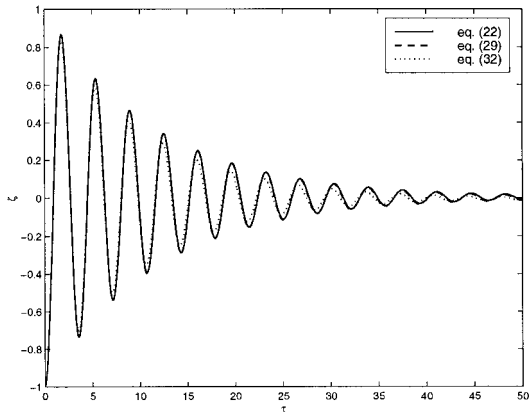

(2b) Re = 200

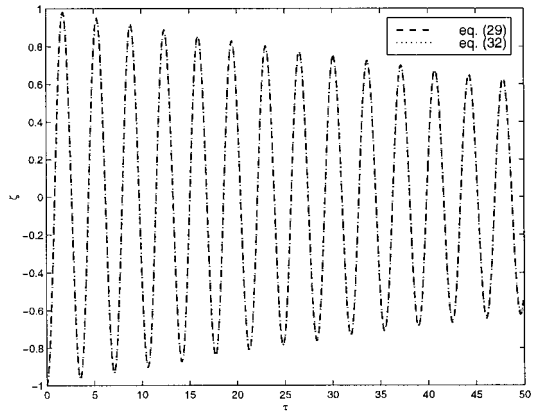

(2c) Re = 2000

Figure 2. Decay of deep water solutions at different Reynolds numbers.

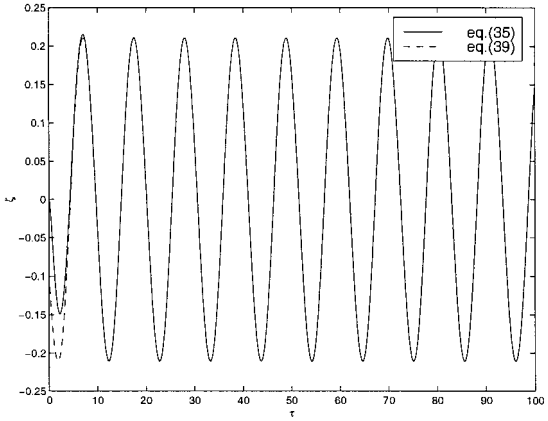

(3a) Re = 2

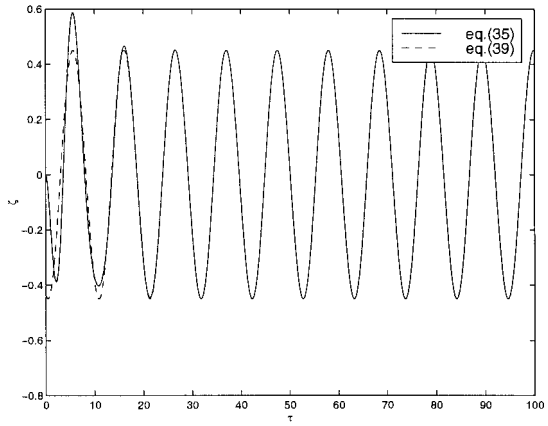

(3b) Re = 20

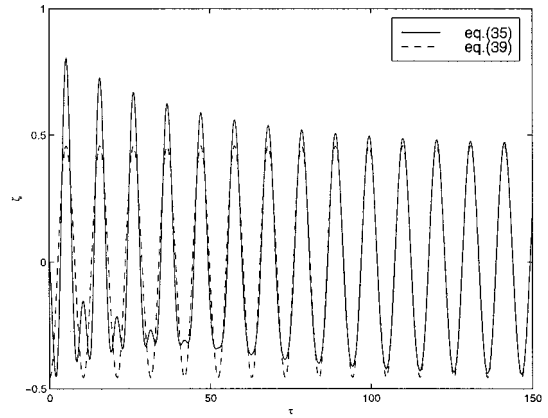

(3c) Re = 200

Figure 3. Wave elevation history with $\omega = 0{\cdot}5\omega_1$.

$$a_{2n-1} = -\frac{4\omega^2 b}{l k_{2n-1}^2} \frac{\lambda^2}{\lambda^2 + \omega^2} \qquad n = 1,\ 2,\ \ldots \tag{34}$$

while all the even terms are zero. Substituting this in (19), we obtain

$$\eta = -\frac{2\omega^2 b}{\pi \mathrm{i} \nu l} \sum_{n=1}^{\infty} \frac{\tanh\ k_{2n-1} d}{k_{2n-1}} \int_{\Gamma} \frac{\tanh\ \alpha_{2n-1} d}{C_{2n-1}} \frac{\lambda^2}{\lambda^2 + \omega^2} \mathrm{e}^{\lambda t}\, \mathrm{d}\lambda\ \cos\ k_{2n-1}(x + l/2). \tag{35}$$

One special case of Equation (35) is $\nu \to 0$. We can then establish that the poles of the integrand are at

$$\lambda = \pm \mathrm{i}\omega_{2n-1} = \pm \mathrm{i}\sqrt{g k_{2n-1}\ \tanh\ k_{2n-1} d} \quad n = 1,\ 2,\ \ldots \tag{36}$$

and

$$\lambda = \pm \mathrm{i}\omega.$$

It follows that

$$\eta = \frac{4\omega^2 b}{l} \sum_{n=1}^{\infty} \frac{\tanh\ k_{2n-1} d}{k_{2n-1}} \left(\frac{\cos\ \omega_{2n-1} t - \cos\ \omega t}{\omega^2 - \omega_{2n-1}^2} \right) \cos\ k_{2n-1}(x + l/2). \tag{37}$$

If we had started the analysis with $\nu = 0$ at the beginning, the last terms in Equations (1a) and (1b) would have been dropped and Equation (2c) should have been deleted because the zero shear force is automatically satisfied when $\nu = 0$. As a result, the problem can be solved using ϕ alone with A_n being obtained from Equation (14b) in which $B_n = 0$ and $\nu = 0$. Thus

$$A_n = -a_n/(\lambda^2 + k_n g\ \tanh\ k_n d). \tag{38}$$

If we use this with Equations (12a) and (34), and $\eta = -\phi_t/g$, we can see that the result is identical to (37). In fact, the same conclusion applies to Equation (22). The interesting point here is that when viscous flow passes a rigid body the solution of the Navier-Stokes equations does not tend to potential flow when $\nu \to 0$, if the no-slip condition is imposed. But for the free surface flow considered in this analysis, in which the zero shear force condition is imposed on all the surfaces, including the solid boundary, the wave elevation in viscous flow tends to the result in inviscid flow when $\nu \to 0$. Furthermore, from Equations (13b), (16) and (17), we can see that A_n tends to (38) and B_n tends to zero as $\nu \to 0$. This confirms that when viscosity tends zero the entire flow field in this case tends to the potential flow.

Another special case of Equation (35) corresponds to $t \to \infty$. It can be speculated that the poles of the integrand due to C_{2n-1} have negative real parts. Although it is not easy to prove this rigorously here, the physics of the problem suggests that the natural modes of oscillation will diminish due to the viscosity. This is supported by the deep water analysis above (the appendix showing explicitly within the region considered there that the non-zero poles $\sigma_i = -1 + \gamma_i^2$ of Equation (23) have negative real parts). Thus, as $t \to \infty$, we have to consider only the poles at $\lambda = \pm \mathrm{i}\omega$ in Equation (35). This yields

$$\eta = -\frac{2\omega^2 b}{\nu l} \sum_{n=1}^{\infty} \frac{\tanh\ k_{2n-1} d}{k_{2n-1}} \mathfrak{Re} \left(\frac{\lambda\ \tanh\ \alpha_{2n-1} d}{C_{2n-1}} \right)_{\lambda = \mathrm{i}\omega} \cos\ k_{2n-1}(x + l/2). \tag{39}$$

But if we let $\nu = 0$ before taking $t = \infty$, Equation (35) will not tend to (39) but to (37). Mathematically this means

$$\lim_{t\to\infty}\lim_{\nu\to 0}\eta \neq \lim_{\nu\to 0}\lim_{t\to\infty}\eta. \tag{40}$$

This behaviour is analogous to that of a single degree of freedom damped oscillator, subject to harmonic excitation from a state of rest at $t = 0$. It is also worth emphasising that the lower the viscosity is the longer it will take before Equation (39) becomes valid.

Extensive results for inviscid flow have been provided in various publications [12, 13]. As discussed above, at small ν, the result from the present analysis will be close to that from the potential flow formulation. Thus the discussion here will focus on flow of relatively high viscosity.

Calculations are again undertaken for a tank with $l = 2d$. Figure 3 gives results for the wave elevation at $x = l/2$ obtained from Equations (35) and (39), for an excitation frequency $\omega = 0{\cdot}5\omega_1$, where the natural frequency of the lowest mode is given by $\omega_1\sqrt{d/g} = \sqrt{k_1 d\ \tanh\ k_1 d} = 1{\cdot}20$. At lower Reynolds number Re $= 2$, Figure 3a shows that the result from Equation (35) tends to that from Equation (39) almost immediately. At Re $= 20$, the natural modes in Figure 3b still decay sharply but the steady wave amplitude is higher. At Re $= 200$, the effect of the first natural mode is evident in Figure 3c, oscillating at a frequency $\omega_1 = 2\omega$. The mode will decay and the result from Equation (35) will tend to that from Equation (39) as time increases, The case in Figure 4 is similar to that in Figure 3, with the only difference being that the excitation frequency is set at the natural frequency, or $\omega = \omega_1$. Apart from the wave having a larger amplitude, the behaviour of the results in Figures 4a and 4b is quite similar to that in Figures 3a and 3b. Major differences can be seen, however, between Figure 4c and Figure 3c. Based on the linearized inviscid flow, the wave elevation will tend to infinity eventually. But here due to the effect of viscosity, the wave amplitude will tend to a steady value. In reality the large wave in the tank will overturn and break. The result here clearly shows that viscosity may have some important effect on wave breaking. If the viscosity is high enough it will damp away the natural modes before the resonant wave becomes sufficiently large to cause breaking. But this may not be relevant to a fluid like water, because its viscosity may be too low to have a marked effect directly on the wave decay. Figure 5 gives corresponding results for an excitation frequency $\omega = 1{\cdot}5\omega_1$. In Figure 5c the contribution from the first natural mode is clearly visible; this will diminish as time increases.

5. Conclusions

The paper has obtained results which demonstrate the interaction between a free surface and unsteady viscous flow, One particular feature noted here is that when a no-shear force condition is imposed on the boundary, the solution of the viscous flow tends to that of the potential flow. This is different from the case where a no-slip condition is imposed on the boundary, However, whether the no-shear force condition has any physical significance is not clear at this stage. Further work is clearly required to resolve the issue of the boundary condition at the intersection. In this context, the work by Somalinga and Bose [14] should be mentioned, which appeared when this paper was being revised. The numerical results provided in the paper are mainly at low Reynolds number, or for a highly viscous fluid; as for fluid of small viscosity, such as water, this type of flow can be captured well by the potential flow theory. It is clear, however, what has been achieved in this paper is quite modest. The real challenge is when turbulence has been developed. In this case it can be expected that the interaction between the free surface wave and viscosity will be important even for fluid of low viscosity.

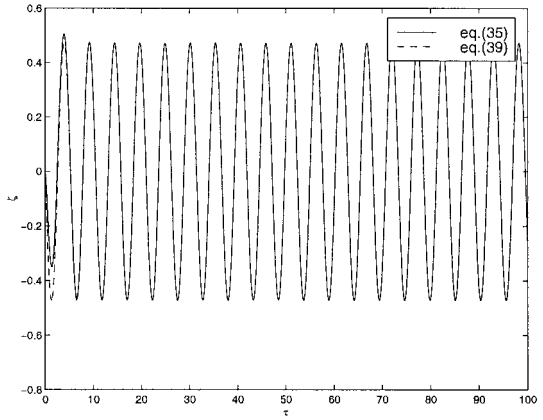

(4a) Re = 2

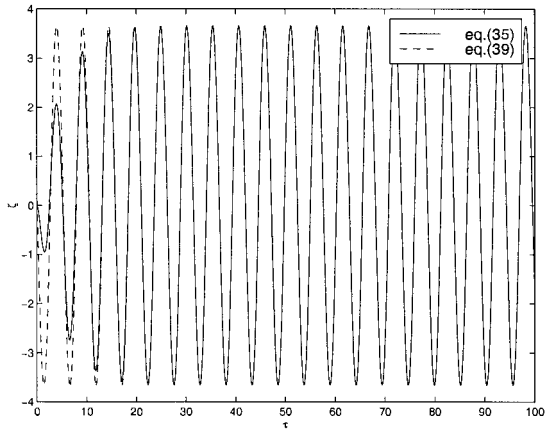

(4b) Re = 20

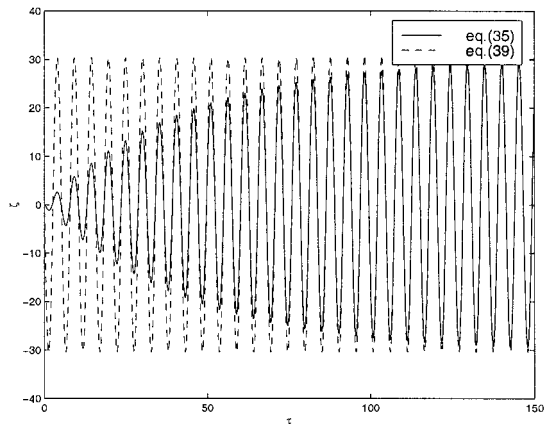

(4c) Re = 200

Figure 4. Wave elevation history with $\omega = \omega_1$.

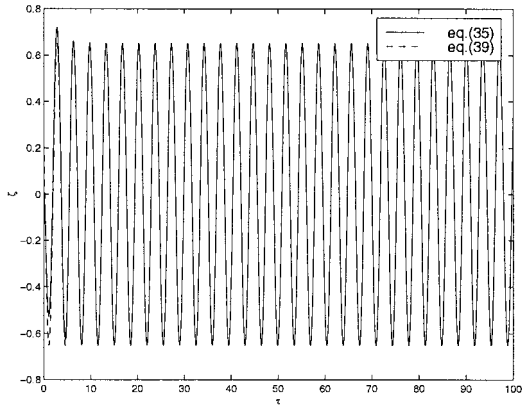

(5a) Re = 2

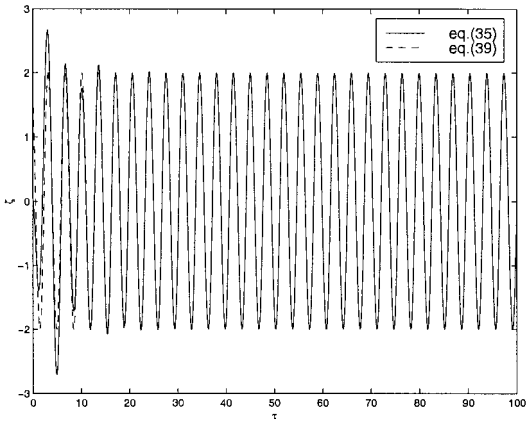

(5b) Re = 20

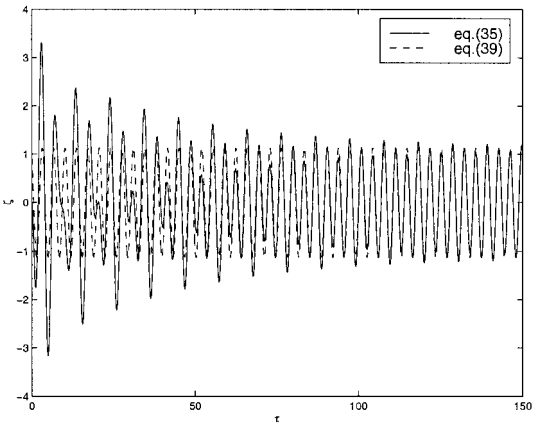

(5c) Re = 200

Figure 5. Wave elevation history with $\omega = 1{\cdot}5\omega_1$.

Appendix: Coefficients for the partial fraction expansion

The complex coefficients A_1 and A_2 in Equation (26) may be written down using the properties of the roots of Equation (27), γ_1, γ_2 and their conjugates. Writing $\gamma_{1R} = \mathfrak{Re}(\gamma_1)$, $\gamma_{1I} = \mathfrak{Im}(\gamma_1)$ and similarly for γ_2, we can obtain

$$\mathfrak{Re}A_1 = -\frac{2}{\Delta}\gamma_{1R}, \quad \mathfrak{Re}A_2 = \frac{2}{\Delta}\gamma_{1R}, \quad \mathfrak{Im}A_1 = -\frac{2\gamma_{1R}^3 + 1}{\gamma_{1R}\gamma_{1I}\Delta}, \quad \mathfrak{Im}A_2 = -\frac{2\gamma_{1R}^3 - 1}{\gamma_{1R}\gamma_{2I}\Delta},$$

where

$$\Delta = 4(6\gamma_{1R}^2 + 1)(2\gamma_{1R}^2 + 1) - 4(\kappa + 1).$$

Other relationships which may be found are:

$$|\gamma_1|^2|\gamma_2|^2 = \kappa + 1;$$

$$\gamma_{1I}^2 = 1 + \gamma_{1R}^2 - \frac{1}{\gamma_{1R}}, \quad \gamma_{2I}^2 = 1 + \gamma_{1R}^2 + \frac{1}{\gamma_{1R}}, \quad \gamma_{1R} + \gamma_{2R} = 0.$$

The second and third of these identities suggest that the roots of Equation (27) are complex conjugate pairs if

$$1 + \gamma_{1R}^2 - \frac{1}{|\gamma_{1R}|} > 0.$$

Following the standard analytical procedure for solving a cubic equation, we can establish that this inequality leads to $|\gamma_{1R}| > 0{\cdot}682327804$. With the help of the four identities given above it can be shown that this further leads to $\kappa > 0{\cdot}581412180$. Furthermore, in support of the comments following Equation (38), it is seen that

$$\mathfrak{Re}[\gamma_i^2 - 1] = \gamma_{iR}^2 - \gamma_{iI}^2 - 1 = -2 \pm 1/\gamma_{1R} < -0{\cdot}534428768, \qquad i = 1,\ 2.$$

The roots γ_1, γ_2 and the coefficients A_1 and A_2 have relatively simple forms for the case $\kappa = 7$:

$$\gamma_1 = -1 + \mathrm{i}\sqrt{3}, \quad \gamma_2 = 1 + \mathrm{i}, \quad A_1 = \frac{1}{26} - \mathrm{i}\frac{\sqrt{3}}{156}, \quad A_2 = \frac{-1}{26} - \mathrm{i}\frac{3}{52}.$$

Acknowledgement

This work was supported by EPSRC Grants GR/L24083 at University College London and GR/L24090 at the University of Oxford, through the MTD Managed Programme in Marine Computational Fluid Dynamics.

References

1. M. J. Lighthill, *Waves in Fluids*. Cambridge: CUP (1978) 504 p.
2. T. Sarpkaya and M. Issacson, *Mechanics of Wave Forces on Offshore Structures*. New York: Van Nostrand (1981) 651 p.

3. R. W. Yeung and X. Yu, Wave-structure interaction in a viscous fluid. *Fourteenth Int. Conf. on Offshore Mech & Arctic Eng*, Copenhagen (Denmark) (1995).
4. C. C. Mei, *The Applied Dynamics of Ocean Surface Waves*. New York: Wiley-Interscience (1983) 740 p.
5. H. Lamb, *Hydrodynamics* (6th edition). Cambridge: CUP (1976) 738 p.
6. Q. Chen, E. Rame and S. Garoff, The velocity field near a moving contact line. *J. Fluid Mech*. 337 (1997) 49–66.
7. E. A. Cerda and E. L. Tirapegui, Faraday's instability in viscous fluid. *J. Fluid Mech*. 368 (1998) 195–228.
8. C. Y. Loh and H. Rasmussen, A numerical procedure for viscous free surface flow. *Appl. Num. Math*. 3 (1987) 479–495.
9. T. B. Benjamin and F. Ursell, The stability of the plane free surface of a liquid in a vertical periodic motion. *Proc. R. Soc. London* A225 (1954) 505–515.
10. G. X. Wu and R. Eatock Taylor, Finite element analysis of two-dimensional non-linear transient water waves. *Appl. Ocean Res*. 16 (1994) 363–372.
11. M. Abramowitz and I. A. Stegun, *Handbook of Mathematical Functions*. New York: Dover (1965) 1043 p.
12. O. M. Faltinsen, A numerical non-linear method of sloshing in tanks with two-dimensional flow. *J. Ship Res*. 18 (1978) 224–241.
13. G. X. Wu, Q. W. Ma and R. Eatock Taylor, Numerical simulation of sloshing waves in a 3D tank based on a finite element method. *Appl. Ocean Res*. 20 (1998) 337–355.
14. S. Somalinga and A. Bose, Numerical investigation of boundary conditions for moving contact line problems. *Phys. Fluids* 12 (2000) 499–510.